Flavanthrone – new ligand with accessible radical anion and dianion states. Preparation of zwitter-ionic {(Cp2V)2(Flavanthrone)} and {(Cp2V)2(Chloranil)} complexes

Journal:	*New Journal of Chemistry*
Manuscript ID	NJ-ART-03-2020-001208.R1
Article Type:	Paper
Date Submitted by the Author:	11-May-2020
Complete List of Authors:	Konarev, Dmitri; Institute of Problems of Chemical Physics RAS, Andronov, Mikhail ; Institute of Problems of Chemical Physics RAS, Chernogolovka, Moscow region, 142432 Russia, Kinetics and Catalysis; Moscow State University, Leninskie Gory,119991 Moscow, Russia Batov, Mikhail; Moscow State University, Kuz`min, Alexey; Institute of Solid State Physics RAS, Khasanov, Salavat; Institute of Solid State Physics RAS, Shestakov, Alexander; Institute of Problems of Chemical Physics RAS Otsuka, Akihiro; Kyoto University - Yoshida Campus, Department of Chemistry; Research Center for Low Temperature and Materials Sciences Yamochi, Hideki; Kyoto University, Kitagawa, Hiroshi; Kyoto University, Department of Chemistry Lyubovskaya, Rimma; Institute of Problems of Chemical Physics RAS,

Journal Name

ARTICLE

Received 00th January 20xx,

Accepted 00th January 20xx

DOI: 10.1039/x0xx00000x

www.rsc.org/

Flavanthrone – new ligand with accessible radical anion and dianion states. Preparation of zwitter-ionic $\{(Cp_2V)_2(Flavanthrone)\}$ and $\{(Cp_2V)_2(Chloranil)\}$ complexes

Dmitri V. Konarev,*[a] Mikhail G. Andronov,[a,c] Mikhail S. Batov,[a,c] Alexey V. Kuzmin,[b] Salavat S. Khasanov,[b] Alexander F. Shestakov,[a,c] Akihiro Otsuka,[d,e] Hideki Yamochi,[d,e] Hiroshi Kitagawa,[d] and Rimma N. Lyubovskaya[a]

Dye flavanthrone (Vat yellow 1) can be reduced to radical anions and dianions crystallized in form of $\{Crypt(Na^+)\}(Flavanthrone^{\bullet-})\cdot 2C_6H_4Cl_2$ (**1**), $(Bu_4P^+)_2(Flavanthrone^{2-})\cdot 0.5C_6H_4Cl_2$ (**2**), and $(Bu_4P^+)_2(Flavanthrone^{2-})$ (**3**) salts, where $\{Crypt(Na^+)\}$ is sodium cryptate[2.2.2]. The reduction of flavanthrone is accompanied by elongation of the carbonyl C=O bonds and shortening of the C-C(O) bonds. Reduction is manifested in optical spectra by essential (more than 200 nm) red shift of the intense band of pristine flavanthrone at 440 nm. A new intense band appears for the flavanthrone$^{\bullet-}$ radical anion at 960 nm in the NIR range but this band decreases in intensity for dianion salts **2** and **3**. Salt **1** contains flavanthrone$^{\bullet-}$ chains of three types in which they are bonded by the C=O···H hydrogen bonds of 2.26-2.53 Å length. Although direct π-π interactions between flavanthrone$^{\bullet-}$ (S = 1/2) are absent, hydrogen bonds between them provide weak antiferromagnetic coupling of spins in the flavanthrone$^{\bullet-}$ layers with Weiss temperature of -5 K. Flavanthrone^{2-} dianions are diamagnetic and EPR silent. Interaction of flavanthrone with two equivalents of vanadocene yields zwitter-ionic $\{(Cp_2V^+)_2(Flavanthrone^{2-})\}\cdot 2C_6H_4Cl_2$ (**4**) complex bonded by short V-O(flavanthrone) bonds. These molecules are packed in uniform stacks with effective π-π interaction between flavanthrone^{2-} units (having the interplanar distance of 3.38 Å). Paramagnetic V^{III} centers with S = 1 spin state are separated in **4** by diamagnetic flavanthrone^{2-} dianions and show weak magnetic coupling with Weiss temperature of -5 K. Zwitter-ionic $\{(Cp_2V^+)_2(QCl_4{}^{2-})\}$ complex (**5**) with smaller diamagnetic chloranil^{2-} spacer shows slightly stronger magnetic coupling with Weiss temperature of -7 K. Modeling of magnetic behavior of **4** and **5** by the appropriate van Vleck equation indicates stronger magnetic coupling between V^{III} in **5** (J = -3.3 cm^{-1}) in comparison with **4** (J = -2.0 cm^{-1}).

Introduction

Organic dyes can be used not only as colorants for fabrics and clothes[1] but now they find application as new electronic materials, materials for rechargeable batteries, and photo- and semiconductors.[2] These dyes are capable of redox transitions and, therefore, unpaired electrons can be introduced into these dyes. Such radical anion species potentially can manifest high conductivity at their appropriate packing in a crystal or participate in magnetic coupling of spins. The dyes having hetero atoms such as carbonyl and/or hydroxy oxygen can coordinate transition metals. Their ability to form radical anion and dianion species as well as in some cases possibility of their deprotonation can essentially modify optical and magnetic properties of dye ligands as well as possible ways of coordination of transition metals to them. As an example, indigo and thioindigo can form radical anions and dianions in solution[3] and solid state[4]. Recently radical anion salt

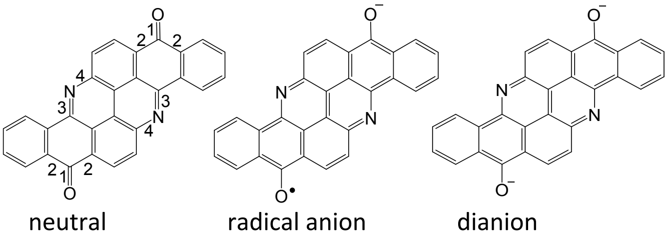

Scheme 1. Molecular structure of neutral flavanthrone and its radical anion and dianion forms.

---

[a] Institute of Problems of Chemical Physics RAS, Chernogolovka, Moscow region, 142432 Russia;
[b] Institute of Solid State Physics RAS, Chernogolovka, Moscow region, 142432 Russia;
[c] Moscow State University, Leninskie Gory,119991 Moscow, Russia;
[d] Division of Chemistry, Graduate School of Science, Kyoto University, Sakyo-ku, Kyoto 606-8502, Japan;
[e] Research Center for Low Temperature and Materials Sciences, Kyoto University, Sakyo-ku, Kyoto 606-8501, Japan.

*Electronic supplementary information (ESI) available: IR spectra of pristine compounds and compounds **1**-**5**, figures with structure of salts **2** and **3**, UV-visible-NIR spectrum of **3**, data of SQUID measurements for compounds **1**, **4** and **5**. CCDC numbers are 1985695-1985698 and 1985700. For ESI and crystallographic data in CIF or other electronic format see DOI: …..*

{cryptand[2.2.2](K)}$_6${*trans*-indigo}$_7$·5.5$C_6H_4Cl_2$ of indigo was obtained in a crystalline form, and it was shown that indigo$^{•–}$ can magnetically interact through short hydrogen bonds.[4c] Coordination of transition metals to neutral or dianionic indigo and thioindigo can change conformation from *trans* to *cis*.[4a, 4b, 5e, 5g] In this case metal centers coordinate simultaneously to two oxygen atoms of the dyes in the complexes with chromium pentamethylcyclopentadienyl[3a,b] or titanium(IV) and indium(III) phthalocyanines[5g]. Deprotonation of indigo opens an additional way to the formation of coordination complexes with one or two metal centers.[5a-d] Some of these complexes show properties of single molecule magnets,[5d] intense absorption associated with metal-to-ligand charge transfer or reversible charge transfer between two ligands coordinated to one metal center where one of two ligands is a deprotonated *cis*-indigo dianion.[4a]

However, the number of organic dyes studied under reduction and in coordination complexes with transition metals is still rather limited. As we discussed above they are limited mainly to the dyes of indigo type[4,5] or chemically modified molecules based on them (so-called "*N*-indigo" derivatives)[6]. Nevertheless, it is obvious that vat dyes can be reduced to the radical anion and dianion state and potentially they can be involved in coordination complexes with transition metals and lanthanides due to the presence of carbonyl groups, which can be transferred to terminal ketyls ($C^•$–$O^–$) or the $O^–$ groups under reduction. Such groups can efficiently bind to various metal centers.[7]

Flavanthrone is well-known vat dye of anthraquinone type synthesized in 1903.[8] However, later it was practically not studied. Its structure, optical properties in solution and photoconductivity are investigated[9] and several soluble flavanthrone derivatives are obtained for light emitting diods[2d]. Based on optical absorption and cyclic voltammetry it was found that flavanthrone has high electron affinity (EA = 3.6 eV) and high oxidation potential (IP = 6.3 eV).[10] In this study, we demonstrate the reduction of flavanthrone to the radical anions and dianions (Scheme 1) and the isolation of these anions in solid crystalline salts. This allows one to study for the first time molecular structures, optical and magnetic properties of these anions. Reduction of flavanthrone by strong reductant vanadocene (E_{ox} = -0.55 V *vs* SCE in THF)[11] yields formally neutral zwitter-ionic {(Cp_2V^+)$_2$(Flavanthrone$^{2–}$)} complex in which vanadocene coordinates to oxygen atoms of flavanthrone and reduces it to the dianion state. It is shown that other redox-active carbonyl-containing compounds also can form such complexes. For example, chloranil-containing {(Cp_2V^+)$_2$($QCl_4^{2–}$)} complex is obtained allowing one to study the role of π-conjugated molecules in magnetic interaction between two V^{III} centers.

Results and discussion.

a. Synthesis.

Table 1. Composition and charge state of the components in **1-5**.

1	{Crypt(Na^+)}(Flavanthrone$^{•–}$)·2$C_6H_4Cl_2$
2	(Bu_4P^+)$_2$(Flavanthrone$^{2–}$)·0.5$C_6H_4Cl_2$
3	(Bu_4P^+)$_2$(Flavanthrone$^{2–}$)
4	(Cp_2V^+)$_2$(Flavanthrone$^{2–}$)·2$C_6H_4Cl_2$
5	(Cp_2V^+)$_2$($QCl_4^{2–}$)

The composition of the obtained compounds is presented in Table 1. Suitable reagents for selective reduction of flavanthrone to the monoanionic radical state are a combination of sodium fluorenone ketyl and cryptand[2.2.2]. Starting flavanthrone is only poorly soluble in *o*-dichlorobenzene but dissolves completely after the reduction forming deep blue-greenish solution. Slow mixing of this solution with *n*-hexane provides precipitation of the crystals of {Crypt(Na^+)}(Flavanthrone$^{•–}$)·2$C_6H_4Cl_2$ (**1**), the composition of which was determined from X-ray diffraction on single crystal. The reaction of flavanthrone with two equivalents of strong organometallic reductants $NaRe(CO)_5$ and $NaCpCo(CO)_2$ in the presence of two equivalents of tetrabutylphosphonium bromide was also studied. Organometallic reductants were chosen to coordinate the $Re(CO)_5$ or $CpCo(CO)_2$ fragments to the oxygen atoms of the dye. Previously it was shown that flavanthrone can form complexes with iron at electroreduction.[12] Crystals obtained in both syntheses have different shape and unit cell parameters. However, IR spectra and X-ray diffraction analyses show that metal-containing fragments are not introduced into these salts and their difference is only due to different content of solvent molecules. Solvent molecules are present in (Bu_4P^+)$_2$(Flavanthrone$^{2–}$)·0.5$C_6H_4Cl_2$ (**2**) obtained with $NaRe(CO)_5$ and are absent in (Bu_4P^+)$_2$(Flavanthrone$^{2–}$) (**3**) obtained with $NaCpCo(CO)_2$. Therefore, organometallic reagents play only a role of reductants in these reactions and affect crystallization of the salts with no inclusion into the crystals. Interaction of one or two equivalents of vanadocene with flavanthrone provides its dissolution (only partial in case of one equivalent) and the formation of deep blue solution from which the crystals of {(Cp_2V^+)$_2$(Flavanthrone$^{2–}$)} ·2$C_6H_4Cl_2$ (**4**) are obtained. Most probably the 1:1 compound of vanadocene with flavanthrone cannot be isolated (same salt **4** was isolated at a 1: 1 ratio of Cp_2V and flavanthrone). To extend this reaction we also studied the interaction of vanadocene with other carbonyl-containing dyes like indigo, thioindigo and chloranil. In the case of indigo and thioindigo no crystals are formed but the crystals of {(Cp_2V^+)$_2$($QCl_4^{2–}$)} (**5**) are obtained with chloranil. Only the 1:1 and 2:1 coordination complexes of vanadocene with 2,5-dimethoxy-1,4-benzoquinone are known by now for the benzoquinone-type ligands.[13]

b. Optical properties.

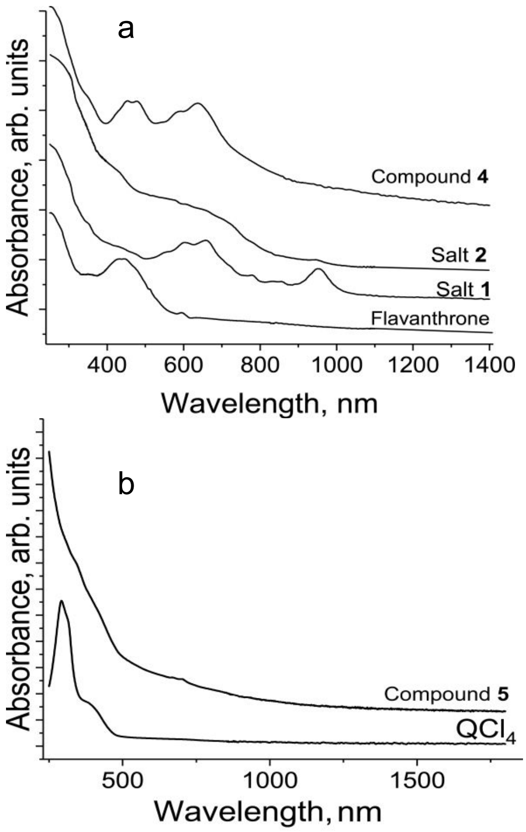

Figure 1. Experimental spectra of compounds obtained based on flavanthrone (**1**, **2** and **4**, left panel) and chloranil (**5**, right panel) in the UV-visible-NIR range.

Pristine flavanthrone classified as dye (Vat yellow 1) has an intense lowest energy absorption band at 440 nm in KBr pellets (Fig. 1a, flavanthrone). The spectrum of flavanthrone studied previously in ethanol has similar features but instead of one band two closely located bands are observed at 440 and 470 nm.[9b] Reduction to the radical anion state shifts an intense absorption band in the visible range, and the magnitude of the red shift is more than 200 nm. As a result, this band appears as a triply split band positioned at 557, 605, and 657 (maximum) nm (Fig. 1a, salt **1**). Moreover, a new intense band appears in the NIR spectrum of **1** with maximum at 960 nm, and weaker bands are observed at 775 and 830 nm (Fig. 1a, salt **1**). Since the formation of the radical anion is accompanied by LUMO population, the new lowest energy band at 960 nm can be attributed to transitions from this partially occupied LUMO to the above located orbitals. The spectra of **2** (Fig. 1a, salt **2**) and **3** (Fig. S9) are similar. The formation of flavanthrone^{2-} dianions in both salts preserves the position of the band near 600-700 nm, and a weaker band is observed as a shoulder at about 430 nm (Fig. 1a, salt **2**). Both bands are strongly broadened (that is observed for both salts), and splitting of the bands is not resolved well in the spectra of salts **2** and **3.** Therefore, the maxima of these bands can be determined only approximately. The band in the NIR range also preserves position at about 940 nm while its intensity essentially decreases (Fig. 1a, salt **2**). Spectrum of $(Cp_2V)_2(Flavanthrone){\cdot}2C_6H_4Cl_2$ (**4**) is also shown in Fig. 1a, compound **4**. It contains two sets of bands at 452, 476 nm and 638, 692 nm in the visible range. The bands at 638 and 692 nm are close to those in the spectra of the salts with flavanthrone^{2-} dianions (**2** and **3**) but they are narrower and better resolved. The intense band of flavanthrone$^{\bullet-}$ observed in the NIR spectrum of **1** is absent in the spectrum of **4** indicating the absence of these species in **4**. Spectrum of pristine chloranil demonstrates a band at 293 nm and a second band is manifested as a shoulder at about 384 nm (Fig. 1b, QCl_4). At the same time $(Cp_2V)_2(QCl_4)$ (**5**) shows no intense bands in the visible range excepting two weak bands at 665 and 695 nm (Fig. 1b, compound **5**).

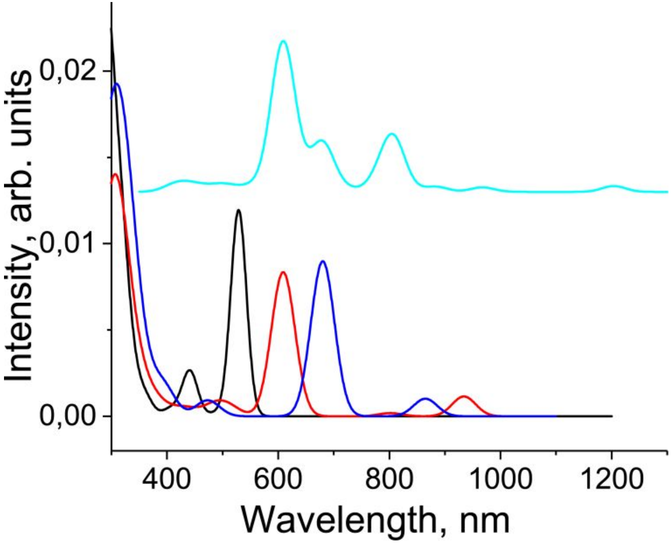

Figure 2. Spectra of pristine flavanthrone according to the TD-DFT calculations of (black curve) as well as flavanthrone radical anion and dianion (red and blue curves, respectively). Spectrum of $(Cp_2V)_2$(Flavanthrone), calculated up to 350 nm, is shown as a cyan curve.

Spectra of neutral flavanthrone, its radical anion, dianion and {$(Cp_2V)_2$Flavanthrone} calculated by using the TD-DFT approach are shown in Fig. 2. Correspondence between the theoretical and experimental spectra is rather good (Figs. 1 and 2). The flat flavanthrone molecule has the C_{2h} symmetry; addition of first and second electrons preserves it and the charge on the O and N heteroatoms (-0.222 and -0.130, respectively) also does not change much for the radical anion (-0.287 and -0.157, respectively) and the dianion (-0.360 and -0.183, respectively). This indicates that approximately 80% of the resulting electron density is accepted by the conjugated π-electron system of flavanthrone.

In pristine flavanthrone HOMO (a_g) consists mainly of unshared pairs of oxygen atoms but HOMO-1 (b_g) and LUMO (a_u) are π-orbitals. The HOMO (a_g) - LUMO (a_u) transition at 679 nm does not appear in the spectrum due to the small moment of transition between σ- and π-orbitals. The most intense band in the visible region at 528 nm originated from the HOMO-1 (b_g) - LUMO (a_u) transition. Partially populated LUMO in flavanthrone$^{\bullet-}$ becomes singly occupied molecular orbital (SOMO). As a result, new low-energy transitions become possible at 934 nm (SOMO (a_u) - LUMO (b_g)) and at 802 nm (SOMO (a_u) - LUMO + 1 (b_g) transition). The most intense transition at 609 nm is the HOMO (b_g) - SOMO (a_u)

analogue of the HOMO - LUMO transition in the neutral system at 679 nm.

LUMO and LUMO + 1 have the same b_g symmetry and close energies in the flavanthrone^{2-} dianion. Therefore, excited terms are described by a superposition of configurations corresponding to various one-electron excitations. This leads to a redistribution of intensities in the spectrum — a less intense transition at 934 nm and a very intense transition at 680 nm. According to the calculations the negative charge on the ligand in {(Cp_2V)$_2$Flavanthrone} is concentrated mainly on the oxygen (-0.202), and nitrogen (-0.151) heteroatoms. The elongation of CO bonds to 1.318 Å in the calculated structure (Fig. S18) indicates a two-electron reduction of the ligand to diol. Four single-filled d - orbitals of two vanadium atoms are located below the HOMO(u) - π-orbital of flavanthrone. The low-energy transitions (above 800 nm) originate mainly from parity allowed transitions from HOMO(u) to the above located unoccupied MOs. The most intense transition at 609 nm, is mixed-type transition to the excited state which is described by superposition of configurations, π-π excitation HOMO(u) - LUMO + 2 (g), and metal-to-ligand transitions. Interestingly, there is a proximity of intense transitions at 609 nm in the radical anion and in the complex (Fig. 2), in the both systems there is small total charge on C and H atoms of the conjugated π electron system.

IR spectra of pristine compounds, salts **1**-**3** and compounds **4** and **5** are shown in Figs. S1-S6 and the positions of the peaks are listed in Tables S1 and S2. All carbonyl containing compounds have absorption bands of high intensity in the 1600-1900 cm^{-1} range characteristic of carbonyl C=O stretching vibrations. For pristine flavanthrone this band appears at 1660 cm^{-1} (Figs. S1). Intense bands which can be attributed to the C-O stretching vibrations in the spectra of the salts are manifested at 1571 cm^{-1} for **1** and 1575 cm^{-1} **2** and **3** whereas the initially intense band of flavanthrone at around 1660 cm^{-1} becomes very weak or completely disappears in the spectra of **1**-**3**. This attribution of the bands is supported by calculations. These data show that reduction provides essential elongation of both C=O bonds even for one-electron reduction of flavanthrone. It can also be concluded that transition from radical anion to dianion is not accompanied by essential elongation of the C-O bond. Presumably, the bands corresponding to the CO stretching vibrations are manifested in the spectrum of (Cp_2V)$_2$(Flavanthrone) (**4**) at 1587 cm^{-1} (intense band) and 1657 cm^{-1}. Thus, though the band of pristine flavanthrone at 1660 cm^{-1} decreases strongly in its intensity, it is still observed in the spectrum of **4**. Intense bands observed in the spectra of **1**-**3** at 1506-1509 cm^{-1} are not found in the spectrum of **4**. Neutral chloranil manifests intense split band at 1680 and 1691 cm^{-1} (Fig. S6). These bands disappear in the spectrum of **5** and the higher energy bands are manifested at 1631 (weak band) and 1420 cm^{-1} (intense band) (Fig. S6).

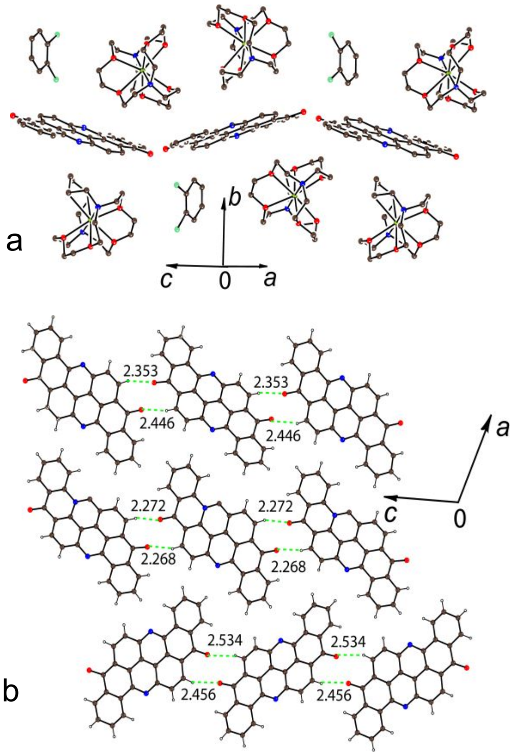

Figure 3. Crystal structure of **1**: views along (a) and on (b) the flavanthrone$^{\bullet-}$ layers arranged in the ac plane and alternating with the Crypt(Na$^+$)-$C_6H_4Cl_2$ layers.

c. Crystal structures.

Salt **1** has layered structure in which the flavanthrone$^{\bullet-}$ layers alternate with the layers composed of Crypt(Na$^+$) and $C_6H_4Cl_2$ (the interlayer distance is about 10.5 Å, Fig. 3a). As a result, no interlayer π-π interactions between flavanthrone$^{\bullet-}$ radical anions are expected in **1**. Radical anions form chains of three types in the layer, each of which is arranged along the *c* axis.

Table 2. Intramolecular bond lengths for flavanthrone molecule in the obtained salts and coordination complex. For the numbering of bonds (indicated in brackets) see Scheme 1.

N	Composition	Length of C=O bonds, Å (1)	Length of C-C(O) bonds, Å (2)	Length of N-C bonds, Å (3) (4)	Length of other C-C bonds, Å
	Flavanthrone[9a]	1.21(3)	1.52(2)	1.30(3) 1.37(3)	1.38(3)
1	{Crypt(Na$^+$)}(Flav$^{\bullet-}$)·$2C_6H_4Cl_2$[a]	1.284(4) 1.355(4)	1.428(5)	1.362(5) 1.342(5)	1.409(5)
2	(Bu$_4$P$^+$)$_2$(Flav^{2-})·$0.5C_6H_4Cl_2$ 1	1.276(4)	1.450(5)	1.363(5) 1.346(4)	1.409(5)
	2 ind. units 2	1.266(4)	1.450(5)	1.360(5) 1.348(4)	1.408(5)
3	(Bu$_4$P$^+$)$_2$(Flav^{2-})	1.271(3)	1.448(3)	1.360(3) 1.348(3)	1.409(3)
4	{(Cp_2V^+)$_2$(Flav^{2-})}·$2C_6H_4Cl_2$	1.312(2)	1.427(3)	1.363(3) 1.339(3)	1.412(3)

[a] Parameters are given only for ordered one of three independent flavanthrone$^{\bullet-}$ units.

The flavanthrone$^{\bullet-}$ radical anions were connected in these chains by C-H···O type intermolecular hydrogen bonds (Fig.

3b). While both oxygen atoms of flavanthrone participated to the hydrogen bond formation in all chains, the interatomic distances showed the difference. The shortest C-O···H-C distance was about 2.27 Å (O···C ≈ 3.10 Å), while they were somewhat longer in two other chains: 2.35, 2.45 Å (3.19 Å) and 2.46, 2.53 Å (3.30 Å). It should be noted that weak hydrogen C-O···H-C bonds are also found for pristine flavanthrone but in this case the O···C distances are about 3.27 Å. Previously, the formation of strong hydrogen C-O···H-N bonds was found in the radical anion salt with the indigo$^{\bullet-}$ radical anions (2.11-2.17 Å).[4c] Essentially shorter hydrogen bonds for indigo$^{\bullet-}$ can be explained by participation of N-H groups in this bonding instead of C-H groups for the hydrogen bonding in **1**. Crystal structures of the dianion salts **2** and **3** are shown in Figs. S7 and S8. In these salts the flavanthrone^{2-} dianions are completely isolated by the bulky Bu_4P^+ cations.

The bond lengths for pristine flavanthrone and its radical anions and dianions are listed in Table 2. In spite of that the bond lengths in flavanthrone were determined with rather low precision,[9a] it is obvious that the C=O double bond is short (1.21(3) Å) and the N-C bonds show different lengths of 1.30(3) and 1.37(3) Å in pristine flavanthrone (Table 2). This feature of bond lengths corresponds well to the canonic form of neutral flavanthrone shown in Scheme 1. The C=O bonds are elongated at reduction, whereas the C-C(O) bonds are shortened to 1.428(5) Å and this length is even closer to the average length of aromatic C-C bonds in flavanthrone$^{\bullet-}$ (1.409(5) Å, Table 2). Homogenization of C-N bond lengths and other bonds in the molecule at reduction indicates increased delocalization of valence electrons. Slight difference between two C-O bonds in flavanthrone$^{\bullet-}$ can be explained by the formation of hydrogen bonds since a longer C-O bond is formed namely with oxygen atoms forming a shorter hydrogen bond (the same situation is observed for all three independent flavanthrone$^{\bullet-}$ units). The formation of dianions does not change essentially the geometry of flavanthrone^{2-} in comparison with the radical anion. The C-O bonds are even shortened in the dianion state (Table 2), since no hydrogen bonds are formed both in **2** and **3**.

Table 3. Geometric parameters of pristine and reference compounds and complexes **4** and **5**.

Compound	Geometric parameters of Cp_2V		Bond length, Å					
	av. C(Cp)-V, Å	Dihedral angle between Cp	C-C bonds C(O)-C(Cl)	C-C bonds C(Cl)-C(Cl)	av C=O bonds	av C-Cl bonds	O(L)-M	C-O-M angle,°
$(Cp_2V)_2$ (Flavantrone) (**4**)	2.284(3)	40.49(4)			1.312(3)		1.971(1)	140.6(2)
$(Cp_2V)_2(QCl_4)$ (**5**)								
Major orientation	2.298(6)	39.7(4)	1.408(5)	1.388(5)	1.324(3)	1.730(3)	1.981(4)	140.7(4)
Minor orientation	2.308(6)	40.7(4)	1.410(5)	1.390(5)	1.326(4)	1.741(3)	1.967(5)	141.0(4)
$(Et_3Sn)_2(QCl_4)$[15a]			1.512(5)	1.319(5)	1.302(5)	1.702(5)	2.075(5)	126.9(4)
$(Fe^{III}Porph^*)_2$ (QCl_4)[15b]			1.406(4)	1.391(4)	1.304(4)	1.733(4)	1.882(4)	134.8(4)
QCl_4[15c]			1.470(4)	1.335(4)	1.191(4)	1.708(3)		
$(MPy^+)(QCl_4^{\bullet-})$[15d]			1.452(4)	1.360(4)	1.245(3)	1.724(3)		-
$C_6(OH)_2Cl_4$ [15e]			1.395(4)		1.352(3)	1.733(4)		

*Porph: 5,10, 15,20-tetrakis(3,5-dimethylphenyl)-2,3,7,8,12,13, 17, 17-octaethylporphyrine; av. average

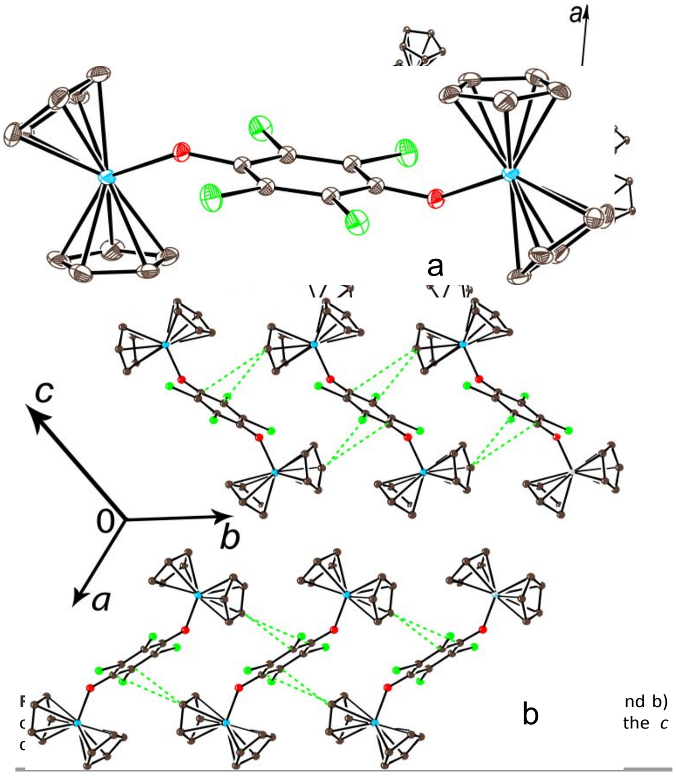

Figure 5. (a) View on the molecular structure of $(Cp_2V)_2$ (QCl_4) in **5**; (b) view on the chains from the $(Cp_2V)_2(QCl_4)$ units arranged along the *b* axis.

Compound **4** contains completely ordered $(Cp_2V)_2$(Flavanthrone) units and disordered *o*-dichlorobenzene molecules. Flavanthrone is able to coordinate transition metals by oxygen atoms and, as a result, it interacts with two equivalents of vanadocene yielding $(Cp_2V)_2$(Flavanthrone) $\cdot 2C_6H_4Cl_2$ (**4**). Compound **4** contains formally neutral zwitter-ionic molecule in which two Cp_2V fragments are bonded to flavanthrone by rather short V-O bonds of 1.971(1) Å length with the C-O-V angle of 140.59°. The intervanadium distance within one molecule is 13.9 Å. Geometry of flavanthrone in **4** is close to those in **1**-**3** excepting the length of the C-O bonds which elongated in comparison with **2** and **3** (Table 2) most probably due to the formation of the O-V coordination bonds.

Similar elongation of the C-O bonds is observed at the formation of the hydrogen bonds in **1**. These molecules are packed in the uniform stacks with effective π-π interaction between the flavanthrone units with the interplanar distance of only 3.38 Å. The planes of flavanthrone are parallel to each other and each flavanthrone forms twelve short C···C contacts of 3.35-3.45 Å length with the neighbors. These data indicate effective π-π interaction between the flavanthrone fragments in **4** (Fig. 4).

In contrast to compound **4**, compound **5** shows multiple disorders of crystal structure. Chloranil unit is positionally disordered in **5** whereas Cp rings of both vanadocene units are rotationally disordered. The latter type of disorder is characteristic of vanadocene[14]. Fig. 5 shows only the positions with major occupancies for chloranil and Cp rings. Interaction of chloranil with two vanadocene molecules produces formally neutral zwitter-ionic $(Cp_2V)_2(QCl_4)$ complex. This complex is formed by the coordination of vanadium to oxygen atoms of chloranil with the formation of rather short O-V bonds of 1.967(5) and 1.981(4) Å length for two different positions of the chloranil fragment. The C-O-V angles are equal to 141.0 and 140.7^o and these values are close to those in **4**. The intervanadium distance is equal to 9.00 Å (this distance is shorter than that in **4** with larger flavanthrone spacer). In the case of smaller chloranil spacer, large Cp_2V groups do not allow close approach of the chloranil planes to each other and effective π-π interaction between them is absent. Only several C(Cp)···Cl, C(QCl_4) contacts are formed (Fig. 5b).

The formation of $(Cp_2V)_2(QCl_4)$ complex **5** is accompanied by essential elongation of the initially double C=O bonds (from 1.191(4) Å) to 1.324(3)-1.326(4) Å indicating the reduction of chloranil at the interaction with vanadocene. Initially chloranil contains single C(O)-C(Cl) bonds and double C(Cl)-C(Cl) bonds according to their length (Table 3). Reduction equalizes these bonds which have rather close length in **5** (1.408(5) and 1.388(5) Å). Similar bond lengths are found in the $(Fe^{III}Porph^*)_2(QCl_4)$ units containing QCl_4^{2-} dianions.[15b] In the limited case all bonds are equalized in the phenylene ring of $C_6(OH)_2Cl_4$[14e] which is a protonated form of QCl_4^{2-} (Table 3).

d. Magnetic properties.

Magnetic properties of salt **1** were studied by SQUID and EPR techniques. Effective magnetic moment of **1** is 1.69 μ_B at 300 K indicating contribution from one non-interacting S = 1/2 spin per radical anion. Reciprocal molar magnetic susceptibility maintains linearity nearly in all studied temperature range allowing the estimation of Weiss temperature of -5 K indicative of weak antiferromagnetic coupling of spins (Fig. 6a). Effective magnetic moment is linear in the 20-300 K range and the decrease of magnetic moment is observed below 20 K due to antiferromagnetic interactions (Fig S10). The absence of direct π-π interaction between the flavanthrone$^{\bullet-}$ radical anions allows one to assume that coupling occurs through weak hydrogen bonds (of the 2.27-2.53 Å lengths). It should be noted that in previously studied $\{$cryptand[2.2.2](K)$\}_6\{$*trans*-indigo$\}_7 \cdot 5.5C_6H_4Cl_2$ salt with indigo$^{\bullet-}$ much shorter hydrogen bonds are formed (of the 2.11-2.17 Å length) and that, in turn, provides stronger magnetic coupling of spins with Weiss temperature of -14 K.[4c] Therefore, shorter hydrogen bonds in organic systems with spins can lead to stronger magnetic coupling.

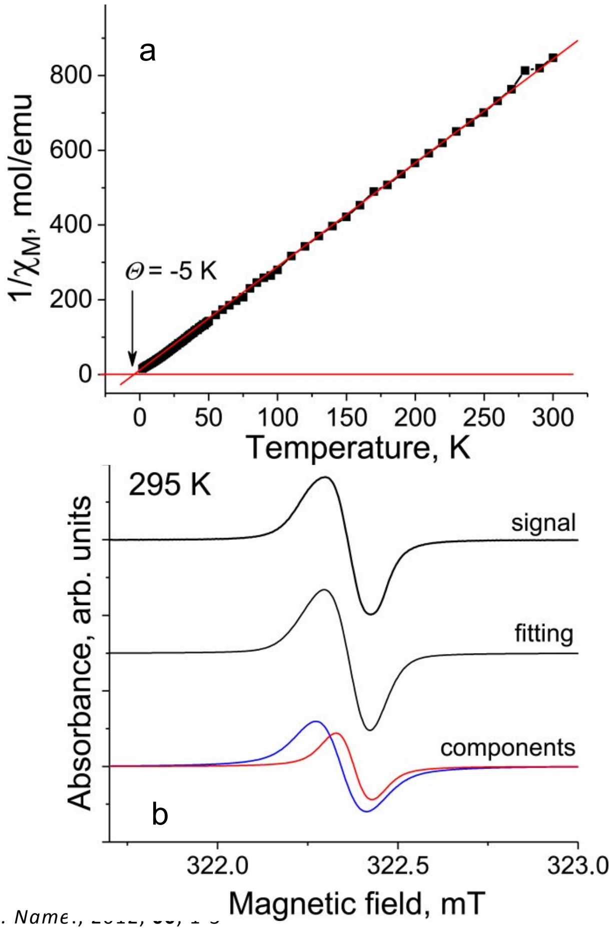

Figure 6. Magnetic data for polycrystalline salt **1**: temperature dependencies of reciprocal molar magnetic susceptibility (a); EPR spectrum at 295 K (b).

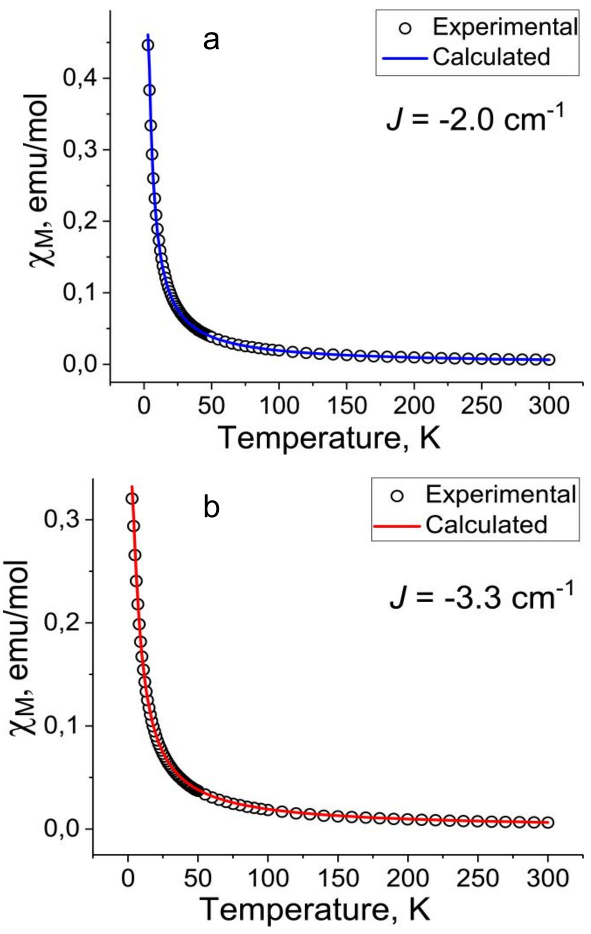

Figure 7. Temperature dependence of molar magnetic susceptibility of polycrystalline compounds **4** (a) and **5** (b). The blue and red lines represent the calculated plots for compounds **4** and **5**, respectively with g = 1.8 and J = -2.0 cm^{-1} (**4**) and J = -3.3 cm^{-1} (**5**). See the text.

The presence of S = 1/2 spin on flavanthrone$^{\bullet-}$ is supported by EPR since salt **1** shows a strong narrow asymmetric signal which can be fitted well by two Lorentzian lines with g_1 = 2.0041 and the linewidth (ΔH) of 0.0994 mT, and g_2 = 2.0043 and ΔH = 0.140 mT (red and blue curves in Fig. 6b, respectively). Integral intensity of this signal corresponds approximately to the contribution of one S = 1/2 spin per radical anion. Salts **2** and **3** containing the flavanthrone^{2-} dianions are EPR silent and diamagnetic.

Effective magnetic moment of **4** is equal to 3.98 μ_B at 300 K (Fig. S11). The expected spin-only value for two noninteracting V^{III} centers with S = 1 spin state is 4.00 μ_B. Since the flavanthrone^{2-} dianions are diamagnetic, they do not contribute to magnetic susceptibility of **4**. The temperature dependence of reciprocal molar magnetic susceptibility is linear near in all studied temperature range (1.9-300 K) allowing Weiss temperature of **4** to be determined as -5 K (Fig. S12). The decrease of magnetic moment of **4** below 10 K (Fig. S11) can be attributed to weak antiferromagnetic interactions. Magnetic behavior of **5** is similar but only with effective magnetic moment of 3.88 μ_B at 300 K (Fig. S13) and Weiss temperature of -7 K (Fig. S14). The decrease of magnetic moment of **5** is observed at higher temperatures of about 30 K (Fig. S13) and can be explained by stronger antiferromagnetic coupling of spins observed in **5** in comparison with **4**. Both compounds are EPR silent that is in agreement with the EPR silent state of both flavanthrone and chloranil dianions and integer spin state (S = 1) of vanadium(III) which is also EPR silent.

Susceptibility data for both compounds were modeled using the modified Van-Vleck equation derived from the Heisenberg spin Hamiltonian:

$$H = -\sum_{\langle i,j\rangle} J_{ij} S_i S_j$$

where J_{ij} is the exchange interaction parameter between two spins, S_i and S_j, and the summation operation is performed over the set of unique exchange bonds; $J > 0$ corresponds to ferromagnetic coupling, whereas $J < 0$ indicates antiferromagnetic coupling. The applied model is similar to that used for analyzing magnetic behavior of previously reported[13] dianion-bridged vanadium(III) S = 1 species and provides an excellent fit.

Obtained constants J = –2.0 cm^{-1} (–2.9 K) for **4** and J = –3.3 cm^{-1} (–4.7 K) for **5** (Fig. 7) demonstrate weak antiferromagnetic interactions between vanadium(III) ions in both cases; g-factor was also treated as a fitting parameter and was found to be g = 1.8, in agreement with d^2 electronic configuration of two metal centers. While in compound **4** with flavanthrone^{2-} the coupling value is lower in magnitude as expected for the longer intervanadium distance (around 13.7 Å), magnetic coupling in **5** with shorter chloranil spacer is stronger. A comparison between compound **5** (this paper) and $(Cp_2V)_2(C_8H_8O_4)$,[13] where $C_8H_8O_4$ is 2,5-dimethoxy-1,4-benzoquinone with J = -4.0 cm^{-1} reveals that the presence of four electron-withdrawing chlorine groups lowers orbital energies of the quinonoid molecule and leads to slightly smaller value of J in comparison with the 2,5-dimethoxy-1,4-benzoquinone dianion as a spacer with two methoxy groups. Recent calculations support this general pattern continuing to manifest itself for other d-block binuclear complexes, thus allowing one to finely tune the degree of antiferromagnetic interactions by adding necessary functional groups to the bridging molecule.[16]

Experimental

Materials.

Flavanthrone (>98%) and tetrabutylphosphonium bromide (Bu_4PBr, >99%) were purchased from TCI. Vanadocene (Cp_2V, 95%), cyclopentadienylcobalt dicarbonyl {$CpCo(CO)_2$, 95%} and rhenium carbonyl ($Re_2(CO)_{10}$, 98%) were purchased from Strem. Sodium fluorenone ketyl $(Na^+)(C_{13}H_8O^{\bullet-})$ and sodium cyclopentadienylcobalt dicarbonyl $(Na^+)\{CpCo(CO)_2^-\}$ were obtained as described[17]. Sodium rhenium pentacarbonyl $(Na^+)\{Re(CO)_5^-\}$ was obtained similarly by mixing metallic sodium and $Re_2(CO)_{10}$ in toluene at a 2:1 molar ratio upon heating during one day at 80°C. Reductant was obtained as brown air-sensitive powder. Cryptand[2.2.2] (98%) was purchased from Acros. *o*-Dichlorobenzene ($C_6H_4Cl_2$) was distilled over CaH_2 under reduced pressure; *n*-hexane was distilled over Na/benzophenone. All operations on the synthesis of **1-5** and their storage were carried out in a MBraun 150B-G glove box with controlled atmosphere and water and oxygen content less than 1 ppm. The solvents were degassed and stored in a glove box. KBr pellets for IR- and UV-visible-NIR measurements were prepared in a glove box. Polycrystalline samples of **1-5** were placed in 2 mm quartz tubes in anaerobic conditions for EPR and SQUID measurements and sealed under ambient pressure of argon gas.

Synthesis

Crystals of **1**–**5** were obtained by diffusion technique. A reaction mixture in *o*-dichlorobenzene was filtered into a 1.8-cm-diameter, 50 mL glass tube with a ground glass plug, and then 30 mL of *n*-hexane was layered over the solution. Slow mixing of the *o*-dichlorobenzene solution with *n*-hexane resulted in precipitation of crystals over 1–2 months. The solvent was then decanted from the crystals, and they were washed with *n*-hexane. The compositions of the obtained compounds were determined via X-ray diffraction analysis on single crystal. For each compound, several crystals tested from one synthesis had the same unit cell parameters and, therefore, they can be attributed to a single crystalline phase. Due to high air sensitivity of **1**–**5**, elemental analysis could not be used to determine the composition, because the complexes reacted with oxygen in the air before the quantitative oxidation procedure could be performed.

The crystals of {Crypt(Na^+)}(Flavanthrone$^{\bullet-}$)$\cdot 2C_6H_4Cl_2$ (**1**) were obtained through the reduction of 17 mg of flavanthrone (0.042 mmol) by slight excess of sodium fluorenone ketyl (12 mg, 0.059 mmol) in the presence of one equivalent of cryptand[2.2.2] (16 mg, 0.042 mmol) in 16 mL of *o*-dichlorobenzene. Intense stirring was carried out during 24 hours at 60°C. Flavanthrone completely dissolved to form blue-greenish solution. The solution was cooled down to room temperature and filtered into a glass tube. The crystals were obtained as black blocks with characteristic gold lustre up to $0.6\times0.6\times0.8$ mm^3 in size in 64% yield.

The crystals of $(Bu_4P^+)_2$(Flavanthrone^{2-})$\cdot 0.5C_6H_4Cl_2$ (**2**) were obtained through the reduction of 17 mg of flavanthrone (0.042 mmol) by sodium rhenium carbonyl (30 mg, 0.086 mmol) in the presence of two equivalents of Bu_4PBr (28.3 mg, 0.084 mmol) in 16 mL of *o*-dichlorobenzene. Intense stirring was carried out during 24 hours at 60°C. Flavanthrone completely dissolved to form deep blue solution. The solution was cooled down to room temperature and filtered into a glass tube. The crystals were obtained as black blocks up to $0.3\times0.4\times0.4$ mm^3 in size in 53% yield.

The crystals of $(Bu_4P^+)_2$(Flavanthrone^{2-}) (**3**) were obtained through the reduction of 17 mg of flavanthrone (0.042 mmol) by sodium cyclopentadienylcobalt dicarbonyl (17 mg, 0.084 mmol) in the presence of two equivalents of Bu_4PBr (28.3 mg, 0.084 mmol) in 16 mL of *o*-dichlorobenzene. Intense stirring was carried out during 24 hours at 60°C. Flavanthrone completely dissolved to form deep blue solution. The solution was cooled down to room temperature and filtered into a glass tube. The crystals were obtained as black blocks up to $0.5\times0.5\times0.6$ mm^3 in size in 75% yield.

The crystals of $(Cp_2V)_2$(Flavanthrone)$\cdot 2C_6H_4Cl_2$ (**4**) were obtained through the reduction of 17 mg of flavanthrone (0.042 mmol) by double excess of vanadocene (16 mg, 0.084 mmol) in 16 mL of *o*-dichlorobenzene. Intense stirring was carried out during 24 hours at 60°C. Flavanthrone completely dissolved to form blue solution. The solution was cooled down to room temperature and filtered into a glass tube. The crystals were obtained as black plates up to $0.6\times0.6\times0.2$ mm^3 in size in 82% yield.

The crystals of $(Cp_2V)_2(QCl_4)$ (**5**) were obtained through the reduction of 10.3 mg of chloranil (0.042 mmol) by double excess of vanadocene (16 mg, 0.084 mmol) in 16 mL of *o*-dichlorobenzene. Intense stirring was carried out during 24 hours at 60°C. Chloranil completely dissolved to form solution of light brown colour. The solution was cooled down to room temperature and filtered into a glass tube. The crystals were obtained as black prisms up to $0.4\times0.4\times0.3$ mm^3 in size in 38% yield.

General

UV-visible-NIR spectra were measured in KBr pellets on a Perkin Elmer Lambda 1050 spectrometer in the 250-2500 nm range. FT-IR spectra (400-7800 cm^{-1}) were measured in KBr pellets with a Perkin-Elmer Spectrum 400 spectrometer. EPR spectra were recorded for polycrystalline samples of **1-5** at room temperature (295 K) with a JEOL JES-TE 200 X-band ESR spectrometer. Weighed amount of $Cu^{II}SO_4\cdot 5H_2O$ was a reference sample for comparison of intensity. A Quantum Design MPMS-XL SQUID magnetometer was used to measure static magnetic susceptibility of **1**, **4** and **5** in 1 kOe magnetic field in cooling and heating conditions in the 300 – 1.9 K range. A sample holder contribution and core temperature independent diamagnetic susceptibility (χ_d) were subtracted from the experimental values. The χ_d values were estimated by the extrapolation of the data in the high-temperature range by fitting the data with the following expression: $\chi_M = C/(T - \Theta) + \chi_d$, where C is Curie constant and Θ is Weiss temperature. Effective magnetic moment (μ_{eff}) was calculated with the following formula: $\mu_{eff} = (8\cdot\chi_M\cdot T)^{1/2}$.

X-ray crystal structure determination

The intensity data for the structural analysis of **1**-**4** were collected on an Oxford diffraction "Gemini-R" CCD diffractometer with graphite monochromated MoK_α radiation using an Oxford Instrument Cryojet system. Raw data reduction to F^2 was carried out using CrysAlisPro, Oxford Diffraction Ltd.[18] X-ray diffraction data for **5** were collected on a Bruker Smart Apex II CCD diffractometer with graphite monochromated MoK_α radiation using a Japan Thermal Engineering Co. cooling system DX-CS190LD. Raw data reduction to F^2 was performed using a Bruker SAINT.[19] The structures were solved by direct method and refined by the full-matrix least-squares method against F^2 using SHELX-2018/3.[20] Non-hydrogen atoms were refined in the anisotropic approximation. Positions of hydrogen atoms were calculated geometrically.

Crystal structures of **1-5** were solved at low temperature (90-118 K). In spite of that and slow cooling of the crystals there are disorders in these salts. There are three independent cryptand(Na$^+$) cations and flavanthrone$^{\bullet-}$ radical anions and six solvent $C_6H_4Cl_2$ molecules in **1**. Two of three cryptand(Na$^+$) cations are disordered between two orientations with the 0.709(6)/0.291(6) and 0.628(3)/0.372(3) occupancies. One of six $C_6H_4Cl_2$ molecule is disordered between two orientations with the 0.702(4)/0.298(4) occupancy. Two of three flavanthrone$^{\bullet-}$ contain a disordered C_3H_4 fragment, which deviates in the opposite directions relative to the molecular plane, and have the 0.676(14)/0.324(14) and 0.587(16)/0.413(16) occupancies. Therefore, we excluded two these molecules from the consideration of the geometry of flavanthrone$^{\bullet-}$. There are two independent Bu_4P^+ cations in **2**. One of two cations is disordered between two positions having 0.696(3)/0.304(3) occupancies. There are one independent Bu_4P^+ cation and half of independent flavanthrone^{2-} in **3**. Two of four butyl chains of Bu_4P^+ are disordered between two orientations with the 0.716(5)/0.284(5) and 0.687(6)/0.313(6) occupancies. Only solvent $C_6H_4Cl_2$ molecules are disordered between two orientations with the 0.9497(18)/0.0503(16) occupancies in the crystal structure of **4**. Structure of **5** contains chloranil units positionally disordered with the 0.587(11)/0.413(11) occupancies. There is also rotational disorder of the Cp rings in the vanadocene units (the occupancy of two orientations is 0.543(7)/0.457(7). The latter type of disorder is characteristic of vanadocene.[13] To keep the anisotropic thermal parameters of the disordered atoms within reasonable limits, the displacement components were restrained using SHELXL instructions of ISOR, SIMU and DELU. That resulted in the 3097, 634, 350, 18, 211 restraints used for the refinement of crystal structures of **1-5**, respectively.

Table 4. Crystallographic data and some details of data collection and refinement for **1-5**.

Compound	**1**	**2**	**3**	**4**	**5**
Empirical formula	$C_{58}H_{56}Cl_4N_4NaO_8$	$C_{63}H_{86}ClN_2O_2\,P_2$	$C_{60}H_{84}N_2O_2P_2$	$C_{60}H_{40}Cl_4N_2O_2V_2$	$C_{26}H_{20}Cl_4O_2V_2$
M_r [g·mol^{-1}]	1101.86	1000.72	927.23	1064.62	608.10
Crystal color and shape,	Black block	Black block	Black block	Black plate	Black prism
Crystal system	Monoclinic	Triclinic	Triclinic	Monoclinic	Monoclinic
Space group	$P\,2_1/c$	$P\,\bar{1}$	$P\,\bar{1}$	$P\,2_1/c$	$P\,2_1/c$
a, Å	33.6385(6)	10.4142(6)	10.0315(5)	15.7671(4)	9.1827(4)
b, Å	20.9981(3)	15.4474(15)	11.1650(5)	17.4553(3)	7.7844(3)
c, Å	23.2161(5)	18.1276(16)	12.4225(6)	8.4909(2)	18.3826(8)
α, °	90	89.892(7)	80.100(4)	90	90
β, °	106.835(2)	84.445(6)	73.741(5)	93.019(2)	90.001(4)
γ, °	90	72.298(7)	87.212(4)0	90	90
V, Å^3	15695.7(5)	2763.9(4)	1315.80(12)	2333.62(9)	1314.02(10)
Z	12	2	1	2	2
ρ_{calc} [g/cm^3]	1.399	1.202	1.170	1.515	1.537
μ [mm^{-1}]	0.296	0.172	0.127	0.680	1.140
F(000)	6897	1082	504	1088	612
T [K]	118(2)	109(2)	113(2)	110(2)	90(1)
2Θ, °	59.418	49.996	59.168	56.564	54.200
Reflns measured	145609	22488	11736	26350	12943
Unique reflns	39279	9658	6173	5747	2894
Params/Restraints	2373/3097	815/634	372/350	319/18	265/211
Reflns [F_o>2σ(F_o)]	22637	5462	4254	4603	2679
R_1[F_o>2σ(F_o)]/ wR_2	0.0885/ 0.2372	0.0738 / 0.2036	0.0705/ 0.1795	0.0398/ 0.0989	0.0287/ 0.0705
G.O.F	1.017	1.013	1.036	1.028	1.089
CCDC number	1985695	1985696	1985697	1985698	1985700

Conclusion

It is shown that flavanthrone dye can be reduced selectively to both radical anion and dianion states. Reduction results in elongation of carbonyl C=O bonds and equalization of all other bonds in this molecule. Extension of π-conjugation in the reduced states can be the reason of an essential red shift of the intense low-energy flavanthrone band at 440 nm by more than 200 nm. Flavanthrone$^{\bullet-}$ radical anions are involved in weak hydrogen C-O···H-C bonds formed in the flavanthrone layers with the length of the H···O contacts of 2.27-2.53 Å, and these bonds provide weak antiferromagnetic coupling between the $S = 1/2$ spins of flavanthrone$^{\bullet-}$. At the same time previously we found that essentially shorter hydrogen C-O···H-N bonds formed in the indigo$^{\bullet-}$ layers of the 2.11-2.17 Å length provided stronger magnetic coupling of the indigo$^{\bullet-}$ spins.[4c] It is shown that flavanthrone can form short V-O coordination bonds with two vanadocene (Cp_2V) units. These units transfer two electrons to flavanthrone, forming flavanthrone^{2-} dianions. As a result, a formally neutral zwitter-ionic $(Cp_2V^+)_2$(flavanthrone^{2-}) complex is obtained. Chloranil also forms a similar zwitter-ionic $(Cp_2V^+)_2$(chloranil^{2-}) complex. Shortening of bridge between two paramagnetic V^{III} centers with $S = 1$ spin state results in stronger magnetic coupling of spins. On the whole, this work shows that carbonyl containing vat dyes can be components for the radical anion and dianion salts. Salts with radical anions potentially can manifest promising magnetic and conducting properties. Flavanthrone anions are able to form coordination complexes with transition metals acting as a bridge ligand between two metal centers. We suppose that the radical anion bridge can enhance magnetic coupling between coordinating paramagnetic centers, and that is a prime matter of an ongoing research.

Conflicts of interest

There are no conflicts to declare.

Acknowledgements

The work was supported by the Ministry of Science and Higher education of the Russian Federation (registration number AAAA-A19-119092390079-8) and by the Kyoto University Foundation and the JST (ACCEL) 27 (100150500019) project.

References

1 (a) Handbook of textile and industrial dyeing, Ed. M. Clark, V. 1. Principles, processes and type of dyes, Woodhead Publishing, 2011. ISBN 978-1-84569-695-5; (b) Dyes, General Survey, H. Mustroph, *Ullmann's Encyclopedia of Industrial Chemistry*. Wiley-VCH. 2014, DOI:10.1002/14356007.a09_073. ISBN 3527306730; (c) C. J. Cooksey, *Biotechnic and Histochemistry*, 2007, **82**, 105-125.

2 (a) E. D. Głowacki, G. Voss, N. S. Sariciftci, *Adv. Mater.* 2013, **25**, 6783-6800; (b) O. Pitayatanakul, T. Higashino, T. Kadoya, M. Tanaka, H. Kojima, M. Ashizawa, T. Kawamoto, H. Matsumoto, K. Ishikawa and T. Mori, *J. Mater. Chem. C*, 2014, **2**, 9311-9317; (c) M. Yao, K. Kuratani, T. Kojima, N. Takeichi, H. Senoh and T. Kiyobayashi, *Sci. Rep.* **2014**, *4*, 3650; (d) K.-Y. Law, *Chem. Rev*., 1993, **93**, 449-486; (e) K. Kotwica, P. Bujak, P. Data, W. Krzywiec, D. Wamil, P. A. Gunka, L. Skorka, T. Jaroch, R. Nowakowski, A. Pron and A. Monkman, *Chem. Eur. J.* 2016, **22**, 7978 – 7986; (f) K. Kotwica, P. Bujak, D. Wamil, M. Materna, L. Skorka, P. A. Gunka, R. Nowakowski, B. Golec, B. Luszczynska, M. Zagorska and A. Pron, *Chem. Commun*. 2014, **50**, 11543 – 11546.

3 (a) A. Roessler, D. Crettenand, O. Dossenbach, W. Marte and P. Rys, *Electrochimica Acta*, 2002, **47**, 1989 – 1995; (b) L. -S. Yen and A. J. Bard, *J. Electroanal. Chem.,* 1976, **70**, 157 – 169.

4 (a) D. V. Konarev, S. S. Khasanov, A. V. Kuzmin, A. F. Shestakov, A. Otsuka, H. Yamochi, G. Saito and R.N. Lyubovskaya, *Dalton Trans*., 2016, **45**, 17095 – 17099; (b) D. V. Konarev, S. S. Khasanov, A. F. Shestakov, A. M. Fatalov, A. Otsuka, H. Yamochi, H. Kitagawa and R. N. Lyubovskaya, *Dalton Trans.,* 2017, **46**, 14365 – 14372; (c) D. V. Konarev, L. V. Zorina, S. S. Khasanov, A. Otsuka, H. Yamochi, H. Kitagawa and R. N. Lyubovskaya, *New J. Chem*, 2019, **43**, 7350 – 7354.

5 (a) W. Beck, C. Schmidt, R. Wienold, M. Steinmann and B. Wagner, *Angew. Chem. Int. Ed*., 1989, **28**, 1529 – 1531; (b) J. -Y. Wu, C. -H. Chang, P. Thanasekaran, C.- C. Tsai, T.- W. Tseng, G. -H. Lee, S. -M. Peng and K.- L. Lu, *Dalton Trans.* 2008, 6110 – 6112; (c) P. Mondal, M. Chatterjee, A. Paretzki, K. Beyer, W. Kaim and G. K. Lahiri, *Inorg. Chem*., 2016, **55**, 3105 – 3116; (d) F. -S. Guo and R. A. Layfield, *Chem. Commun*. 2017, **53**, 3130 – 3133; (e) D. V. Konarev, L. V. Zorina, S. S. Khasanov, A. F. Shestakov, A. M. Fatalov, A. Otsuka, H. Yamochi, H. Kitagawa and R. N. Lyubovskaya, *Inorg. Chem*. 2018, **57**, 583 – 589; (f) M. Chatterjee, P. Ghosh, K. Beyer, A. Paretzki, J. Fiedler, W. Kaim and G. K. Lahiri, *Chem. Asian J*. 2018, **13**, 118 – 125; (g) D. V. Konarev, A. V. Kuzmin, A. M. Fatalov, S.S. Khasanov, E. I. Yudanova and R. N. Lyubovskaya, *Chem. Eur. J.* 2018, **24**, 8415 – 8423; (h) W. Kaim and G.K. Lahiri, *Coord. Chem. Rev.,* 2019, **393**, 1 – 8.

6 (a) G. Nawn, K. M. Waldie, S. R. Oakley, B. D. Peters, D. Mandel, B. O. Patrick, R. McDonald and R. G. Hicks, *Inorg. Chem*. 2011, **50**, 9826 – 9837; (b) P. Mondal, S. Plebst, R. Ray, S. M. Mobin, W. Kaim and G. K. Lahiri, *Inorg. Chem.* 2014, **53**, 9348 – 9356.

7 Alkoxo- and aryloxo-derivatives of metals, D. C. Bradley, R. C. Mehrotra, I. P. Rothwell and A. Singh, Academic Press, UK, 2001. ISBN 0-12-124140-8.

8 R. Scholl and H. Berblinger, *Chem. Ber.* 1903, **36**, 3427 – 3445.

9 (a) H. P. Stadler, *Acta Cryst.* 1953, **6**, 540 – 542; (b) R. A. Durie, R. E. Lack and J. S. Shannon, *Aust. J. Chem.* 1957, **10**, 429 – 447; (c) I. Hiroo, *Bull. Chem. Soc. Jpn*., 1954, **27**, 22 – 27.

10 E. D. Głowacki, L. Leonat, G. Voss, M. Bodea, Z. Bozkurt, M. Irima-Vladu, S. Bauer, N. S. Sariciftci, Proc. SPIE-Int. Soc. Opt. Eng. 2011, 8118, 81180M.

11 J. D. L. Holloway and W. E. Geiger Jr., *J. Am. Chem. Soc.* 1979, **101**, 2038 – 2044.

12 (a) T. Bechtold, E. Burtscher, A. Amann and O. Bobleter , *Chem. Soc., Faraday Trans.*, 1993, **89**, 2451 – 2456; (b) B. Thomas and T. Aurora, *J. Electroanal. Chem*. 2006, **591**, 118 – 126.

13 F. Calderazzo, U. Englert, G. Pampaloni and V. Passarelli, *J. Chem. Soc., Dalton Trans.,* 2001, 2891 – 2898.

14 M. Yu. Antipin and R. Boese, *Acta Cryst.* 1996, **B52**, 314 – 322.

15 (a) P. J. Wheatley, *J. Chem. Soc.* 1961, 5027 – 5029; (b) D. Sahoo, A.K. Singh and S.P. Rath, *Eur. J. Org. Chem.* 2016, 3305 – 3313; (c) S. S. C. Chu, G. A. Jeffrey and T. Sakurai, *Acta Cryst.* 1962, **15**, 661 – 671; (d) K. Molčanov, V. Stilinović, A. Šantić, N. Maltar- Strmečki, D. Pajić and B. Kojić-Prodić, *Cryst. Growth Des.* 2016, **16**, 4777 – 4782; (e) T. Sakurai, *Acta Cryst*. 1962, **15**, 443 – 447.

16 G. David, F. Wennmohs, F. Neese and N. Ferre, *Inorg. Chem.* 2018, **57**, 12769 – 12776.

17 (a) D. V. Konarev, S. S. Khasanov, E. I. Yudanova and R. N. Lyubovskaya, *Eur. J. Inorg. Chem.* 2011, 816 – 820; (b) D. V. Konarev, M. G. Andronov, A. V. Kuzmin, S. S. Khasanov, M. S. Batov, A. Otsuka, H. Yamochi, H. Kitagawa and R. N. Lyubovskaya, *Inorg. Chim. Acta*, 2018, **483**, 504 – 509.

18 Crysalis Bruker AXS Inc., Madison, Wisconsin, USA.

19 Bruker Analytical X-ray Systems, Madison, Wisconsin, U.S.A, **1999.**

20 G. M. Sheldrick, *Acta Crystallogr., Sect. A: Fundam. Crystallogr.* 2008, **64,** 112 – 122.

Graphic for TOC

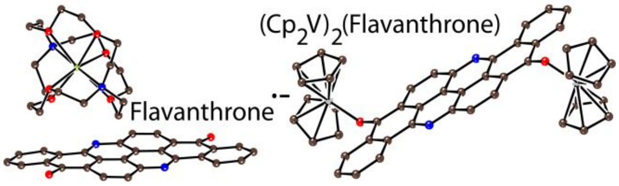

Dye flavanthrone can be reduced to the radical anion and dianions whose molecular structure, optical and magnetic properties are studied. Flavanthrone dianions coordinate to vanadium by oxygen atoms forming zwitter-ionic complex $\{(Cp_2V^+)_2(Flavanthrone^{2-})\}\cdot 2C_6H_4Cl_2$. Related complex $\{(Cp_2V^+)_2(QCl_4^{2-})\}$ shows stronger magnetic coupling between the V^{III} centers in comparison with larger flavanthrone spacer.